



This is the accepted manuscript made available via CHORUS. The article has been published as:

Exchange-correlation contributions to thermodynamic properties of the homogeneous electron gas from a cumulant Green's function approach

J. J. Kas, T. D. Blanton, and J. J. Rehr

Phys. Rev. B **100**, 195144 — Published 26 November 2019

DOI: 10.1103/PhysRevB.100.195144

Exchange-correlation contributions to thermodynamic properties of the homogeneous electron gas from a cumulant Green's function approach

J. J. Kas, T. D. Blanton, and J. J. Rehr Dept. of Physics, Univ. of Washington Seattle, WA 98195 (Dated: October 18, 2019)

Thermodynamic properties of the interacting homogeneous electron gas are calculated using a finite-temperature cumulant Green's function approach over a broad range of densities and temperatures up to the warm dense matter regime $T \sim T_F$, where T_F is the Fermi degenearcy temperature. These properties can be separated into independent particle and exchange-correlation contributions, and our focus here is on the latter. Our approach is based on the Galitskii-Migdal-Koltun and electron number sum-rules from the finite temperature many-body Green's function formalism, together with an extension of the cumulant Green's function to finite-temperature. Previously this approach yielded exchange-correlation energies and potentials in good agreement with quantum Monte-Carlo calculations. Here the method is extended for various thermodynamic quantities including the chemical potential, total energy, Helmholtz free-energy, electronic equation of state, specific heat, and isothermal compressibility, which optionally include spin-dependence. We find that the exchangecorrelation contributions are weakly varying at low temperature but exhibit significant temperature dependence in the WDM regime, as well as a cross-over from exchange- to correlation-dominated behavior. In contrast to the $T=0^+$ limit, we also find that renormalization effects are largely but not completely suppressed at finite temperature. Comparisons with other approaches at various levels of approximation are also discussed.

I. INTRODUCTION

Finite temperature (FT) effects in electronic systems are of both fundamental and practical importance. Physical properties depend strongly on whether the temperature T is large or small compared to the Fermi temperature $T_F \approx 1.84/r_s^2$, which is typically a few eV/ k_B at normal electron densities n = N/V. Here k_B is Boltzmann's constant and $r_s = (4\pi n/3)^{-1/3}$ is the Wigner-Seitz density parameter. [Throughout this work we use Hartree atomic units $m_e = e = \hbar = (4\pi\epsilon_0)^{-1} = k_B = 1$, i.e., energies and temperatures in Hartrees and distances in Bohr, unless otherwise specified. We also suppress arguments of temperature and density unless needed for clarity. At very low temperatures $T \ll T_F$, electrons are nearly degenerate and Fermi liquid behavior is applicable. Recently, however, there has been considerable interest in the warm-dense-matter (WDM) regime where T is of order T_F . This regime is typically encountered in applications ranging from XFEL sources to lasershocked systems, inertial confinement fusion and planetary interiors. 1-3 In WDM, condensed matter becomes partly ionized and exchange effects are significantly reduced. Matter also becomes luminous due to black-body radiation. Thus the nature of exchange and correlation at finite T becomes an important consideration, posing a daunting finite-temperature many-body problem.

Calculations of thermodynamic properties of weakly correlated electronic systems can be obtained from various methods, including quantum Monte Carlo (QMC),^{4–7,9} finite-temperature DFT,^{10–12} and many body perturbation theory (MBPT).^{13–18} Currently QMC is considered to be the most accurate first principles method. However this approach can be computationally intensive and is not routinely available for many ma-

terials. Instead, practical calculations are often based on the FT generalization of DFT. Although in principle, FT DFT is exact, its use in practice depends on the accuracy of FT exchange-correlation functionals. 19-21 Such functionals are typically constructed from fits to QMC calculations for the interacting homogeneous electron gas (HEG).^{4-7,9,22,23} Nevertheless both QMC and DFT have various limitations. For example, there is a paucity of accurate QMC data at very low $T \ll T_F$, and currently available FT exchange-correlation functionals have limited accuracy outside the range of available data and for derived quantities like the specific heat.²⁰ Moreover, these approaches are not designed to address various excited state properties such as optical spectra and inelastic losses at elevated temperatures. ^{25,26} Thus it is desirable to develop alternative approaches. Thermal effects from phonons and other excitations are also generally important in condensed matter, ^{13–15,27,28} but their contributions to the thermodynamics are essentially additive and are not discussed here.

In an effort to address these limitations, we follow an approach within MBPT based on the Green's function (GF) formalism of Martin and Schwinger (MS)²⁹ with a finite-temperature retarded cumulant (RC) Green's function.³⁰ In this approach thermodynamic properties are derived in terms of the Galitskii-Migdal-Koltun (GMK) and electron number sum rules.^{15,29-31} Our aim is to extend the approach for thermal properties of the HEG, for both unpolarized and spin-polarized cases, over a broad range of temperatures including the WDM regime. These properties can generally be separated into independent-particle and exchange-correlation parts. Since the independent-particle contributions for the HEG are known to high numerical accuracy,²⁷ we focus here on exchange-correlation

contributions. 13-15,25,32-34 Although the finite temperature Green's function theory has been known for many years, e.g., from the classic works of Martin and Schwinger (MS)²⁹ and Luttinger and Ward (LW),³⁵ and there have been many studies of low temperature behavior,³⁶ surprisingly little attention has been devoted to its application at temperatures of order T_F . ^{16,30} Formally, the FT GF approach is based on a Matsubara representation of the Green's function which can be analytically continued to the real axis. 13-15 Variational methods such as those based on the LW functional have also been developed.³⁷ In the zero-temperature limit, the theory simplifies. 35,38 Renormalization effects are suppressed and Fermi liquid behavior and the quasi-particle approximation become applicable. 14,35,38,39 Another of our aims here is to assess to what extent these simplifications remain valid at finite T.

In the remainder of this paper Sec. II. describes the formalism used; Sec. III. contains results for several thermodynamic properties of the unpolarized HEG; and Sec. IV., those of the spin-polarized HEG. Sec. V. contains a summary and conclusions.

II. FORMALISM

A. Green's function and spectral function

Green's function methods can be formulated in various ways. Typically the Green's function G is obtained using the Dyson equation $G = G^0 + G^0\Sigma G$, where G^0 is the independent particle Green's function, and Σ is the one-electron self-energy. This equation is also valid at finite temperature. In the GW approximation of Hedin, for example, the self-energy is calculated to leading order the screened Coulomb interaction W^{40} . Thus $\Sigma^{GW} \equiv iGW$ and vertex corrections are neglected. The effects of electron-electron interactions are manifested in the structure of the single-particle spectral function $A_k(\omega)$, which characterizes the energy distribution of a given single particle level k in which G is assumed to be diagonal,

$$A_k(\omega) = -\frac{1}{\pi} \operatorname{Im} G_k(\omega). \tag{1}$$

An attractive alternative to the GW-Dyson equation approach is the retarded cumulant Green's function, which we have recently extended to finite temperature. At T=0 this approach has been applied in a variety of contexts. Anong its advantages the method is formally exact for the model of an isolated electron coupled to bosons, and it generally improves on the GW approximation, 40,47,48 since it implicitly includes vertex corrections and a better description of satellites. Another is that the approach permits a physical interpretation of exchange correlation effects in terms of physical quantities such as dielectric response. In the time domain, the cumulant GF has a pure exponential representation, and

the spectral function is obtained from its Fourier transform

$$G_k(t) = -i\theta(t)e^{-i\varepsilon_k^x t}e^{\tilde{C}_k(t)}, \tag{2}$$

$$A_k(\omega) = -\frac{1}{\pi} \text{Im} \int d\omega \ e^{i\omega t} G_k(t). \tag{3}$$

Here the one-electron energy $\varepsilon_k^x = \varepsilon_k^0 + \Sigma_k^x$ is defined to include the static exchange energy $\Sigma_k^x = \sum_q v_{k-q} n_q$, where $v_q = 4\pi/q^2$ is the bare Coulomb potential, $\varepsilon_k^0 = k^2/2$, and $n_k(T)$ is the temperature dependent occupation number defined in Eq. (11) below. Thus the static-exchange and dynamic correlation contributions are separable, i.e., $C_k(t) = -i\Sigma_k^x t + \tilde{C}_k(t)$. This formalism is similar to that for T = 0, except for the substitution of a finite temperature GW self energy $\Sigma_k^{GW}(T)$.

The cumulant formulation of the Green's function can be justified by the quasi-boson approximation, 40 in which electron-electron interactions are represented in terms of electrons coupled to bosonic excitations. A prescription for the cumulant $\tilde{C}(t)$ can be obtained in analogy to that at T=0, by expanding both the cumulant and Dyson Green's function in terms of the screened Coulomb potential W, and comparing term by term. Carried to all orders the cumulant GF is formally exact. However, as in our original development, 30 we limit the approximation for the cumulant here to first order in W. The retarded cumulant $\tilde{C}_k(t)$ is then obtained in terms of the retarded GW self energy Σ^{GW} , i.e.,

$$\tilde{C}_k(t) = \int d\omega \frac{\gamma_k(\omega)}{\omega^2} (e^{-i\omega t} + i\omega t - 1),$$
 (4)

$$\gamma_k(\omega) = \frac{1}{\pi} \left| \operatorname{Im} \Sigma_k^{GW} (\omega + \varepsilon_k^0) \right|.$$
 (5)

These relations are valid at all temperatures, and their temperature dependence is implicit in that of the selfenergy. 30,47 The FT GW self-energy can be determined at various levels of self-consistency as discussed below. Once the self-energy is obtained, the cumulant kernel $\gamma_k(\omega)$ is given by its imaginary part from Eq. (5). The kernel $\gamma_k(\omega)$ reflects the quasi-boson excitation spectrum, with peaks corresponding to those in the loss function $L(q,\omega) = |\operatorname{Im} \epsilon^{-1}(q,\omega)| \propto |\operatorname{Im} \Sigma_k^{GW}(\omega + \varepsilon_k)|, \text{ as expected}$ on physical grounds. Eq. (4) corresponds to the Landau representation, 40,46,50 which, along with the positivity of $\gamma_k(\omega)$, ensures a positive definite spectral function. The form for the cumulant in Eq. (4) yields a quasi-particle peak of strength $Z_k = \exp(-a_k)$, where Z_k is the renormalization constant, and $a_k = \int d\omega \gamma_k(\omega)/\omega^2$ is the net strength of the satellites. The quasi-particle energy is then $\varepsilon_k = \varepsilon_k^0 + \Delta_k$, where $\Delta_k = \Sigma_k^x + \int d\omega \, \gamma_k(\omega)/\omega$. The Landau form also implies that both $\tilde{C}(0)$ and $(d\tilde{C}(t)/dt)|_{t=0}$ are zero, so the spectral function is always normalized to unity with a first moment given by the unshifted bare one-electron energy ε_k^x .

$$\int d\omega \, A_k(\omega) = 1; \quad \int d\omega \, \omega A_k(\omega) = \varepsilon_k^x. \tag{6}$$

B. Finite T GW Self-energy

As outlined above, the retarded cumulant Green's function is dependent on the retarded one-particle self-energy $\Sigma_k(\omega)$, which can be calculated from MBPT with the Matsubara Green's function.^{15,33} Although more elaborate approximations are possible, here we use the FT GW approximation for $\Sigma_k^{GW}(\omega)$ at the G^0W^0 level, i.e., with the non-interacting Green's function G^0 and the RPA screened interaction $W^0 = \epsilon^{-1}(q,\omega)v_q$, where the dielectric function is given by

$$\epsilon(q,\omega) = 1 + 2v_q \int \frac{d^3k}{(2\pi)^3} \frac{f_{\mathbf{k}+\mathbf{q}} - f_{\mathbf{k}}}{\omega - \varepsilon_{\mathbf{k}+\mathbf{q}} + \varepsilon_{\mathbf{k}}}.$$
 (7)

With these approximations, the self energy corresponds to that for electrons coupled to bosons, with a form similar to the Migdal approximation for electrons coupled to phonons, 33

$$\Sigma^{GW}(\omega; n, T) = \int d\omega' \frac{d^3q}{(2\pi)^3} |\operatorname{Im} W(q, \omega')| \times \left[\frac{f(\varepsilon_{k-q}) + \tilde{N}(\omega')}{\omega + \omega' - \varepsilon_{k-q} + i\delta} + \frac{1 - f(\varepsilon_{k-q}) + \tilde{N}(\omega')}{\omega - \omega' - \varepsilon_{k-q} + i\delta} \right] . (8)$$

Here $\tilde{N}(\omega)=1/(e^{\beta\omega}-1)$ is the Bose factor, which dominates the temperature dependence at high T since $\tilde{N}(\omega)\to k_BT/\omega$. The RPA expression for W^0 is analogous to that often used in zero-temperature GW^0 approximations. The integral for the imaginary part ϵ_2 of $\epsilon(q,\omega)^{52,53}$ in Eq. (7) can be performed analytically and the real part ϵ_1 can then be calculated via a Kramers-Kronig transform. This yields the FT loss function $L(q,\omega)=-\mathrm{Im}\,\epsilon^{-1}(q,\omega)=\epsilon_2/(\epsilon_1^2+\epsilon_2^2)$. For the HEG $L(q>0,\omega)$ exhibits broadened and blue-shifted plasmon-peaks with increasing $T.^{25,53}$

C. Electron number and energy sum-rules

As in the formalism of MS,²⁹ our treatment of the thermodynamics of many-electron systems starts from the grand potential $\Omega(\mu,T)$, as obtained from the grand canonical partition function $\Xi(\mu,T)=\exp(-\beta\Omega)=\mathrm{Tr}\exp[-\beta(H-\mu N)]$, where H is full N-electron Hamiltonian, μ the chemical potential, and $\beta=1/k_BT$. Within MBPT, $\Omega(\mu,T)$ can be expressed in terms of the one-electron Green's function.^{29,35} Thermodynamic properties are then obtained using sum-rules for the total electron number and energy,²⁹ together with thermodynamic identities. Thus all thermodynamic quantities can be derived formally from effective one-electron properties.

First using the relation $N=\partial\Omega/\partial\mu$ the total electron number N in a system of volume V at fixed electron

density n = N/V in the thermodynamic limit is given by

$$N(\mu, T) = \sum_{k} \int d\omega \, A_k(\omega) f(\omega), \tag{9}$$

$$= \sum_{k} n_k(\mu, T). \tag{10}$$

Here $f(\omega) = 1/[e^{\beta(\omega-\mu)} + 1]$ is the Fermi factor, $\mu = \mu(T, n)$ the chemical potential which is determined self-consistently by charge conservation $N(\mu, T) = N$, and

$$n_k(\mu, T) = \int d\omega \, A_k(\omega) f(\omega) \tag{11}$$

is the mean occupation number of state k at finite T. The temperature and chemical potential dependence in $N(\mu, T)$ stems from that in the Fermi factors $f(\mu, T)$ and the Bose factors $\tilde{N}(\omega)$ in the construction of $W(\omega)$, $\Sigma^{GW}(\omega)$, and $A_k(\omega)$.

Next, the Galitskii-Migdal-Koltun (GMK) sum rule is used to obtain the net electronic energy per particle $\varepsilon(T) = E(\mu,T)/N$ for fixed n in the thermodynamic limit. ^{15,29,31} The total energy $E(\mu,T)$ is given by

$$E(\mu, T) = \sum_{k} \int d\omega \, \frac{1}{2} (\omega + \varepsilon_k^0) A_k(\omega) f(\omega). \tag{12}$$

The GMK sum rule is valid for any Hamiltonian with only pair interactions. While the GMK sum-rule depends only on one-particle properties, it is non-variational, and only exact when the true Green's function is known.⁵⁴ A constraint on the approximation for the spectral function is given by the identity $(\partial E/\partial \mu)_T = -T(\partial N/\partial T)_{\mu}$.²⁹

To facilitate the calculations, the sum-rules in Eq. (9) and (12) can be expressed as one-dimensional Fermi integrals over the one-electron density of states per unit volume $g(\omega)$ of the interacting system, and similarly for the electron energy density of states per unit volume $\xi(\omega)$,

$$n(\mu, T) = \int d\omega \, g(\omega) f(\omega),$$
 (13)

$$u(\mu, T) = n\varepsilon(\mu, T) = \int d\omega \, \xi(\omega) f(\omega),$$
 (14)

where

$$g(\omega) = \frac{1}{V} \sum_{k} A_k(\omega), \tag{15}$$

$$\xi(\omega) = \frac{1}{V} \sum_{k} \frac{1}{2} [\omega + \epsilon_k^0] A_k(\omega). \tag{16}$$

However, the usual Sommerfeld expansion techniques for approximating these Fermi integrals at low T are generally inapplicable due to the implicit temperature and chemical potential dependence of $g(\omega)$ and $\xi(\omega)$. These densities of states are compared in Fig. 1 for $r_s = 4$ at T = 0. Note in particular, that the reduction in $g(\omega)$ compared to $g^0(\omega)$ in the RC, GW and PP (plasmon

10

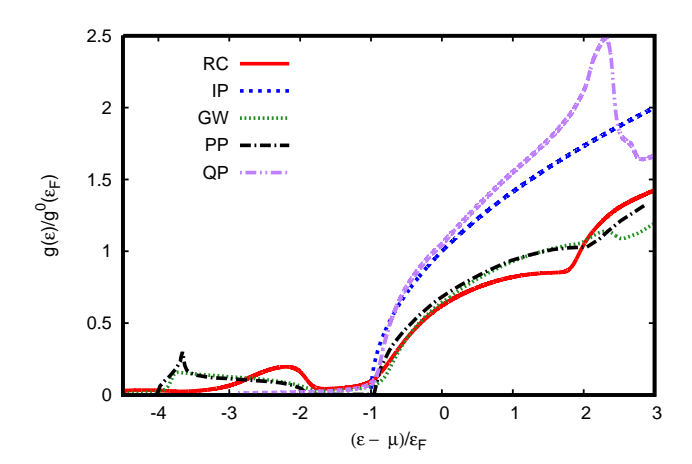


FIG. 1: (Color online) Density of states $g(\varepsilon)$ of the HEG for $r_s = 4$ and T = 0, normalized by that of the independent-particle $g^0(\varepsilon_F)$ at the Fermi energy ε_F . Compared are the densities of states for the retarded cumulant (RC) approach of this work (red), the independent particle (IP) method (blue), the G^0W^0 approach used here (green), the plasmon-pole approximation (PP) of Lundqvist (black),⁵⁵ and the quasi-particle approximation (QP) (violet).

pole) approximations is due to the quasi-particle renormalization factor Z_k and satellites in the spectral function.

Since the independent particle contributions $\mu^0(n,T)$ and $\varepsilon^0(n,T)$ are known quantities, the chemical potential and energy per particle can be decomposed into independent-particle and exchange-correlation parts,

$$\mu(n,T) = \mu^{0}(n,T) + \mu_{xc}(n,T),$$
 (17)

$$\varepsilon(n,T) = \varepsilon^0(n,T) + \varepsilon_{xc}(n,T). \tag{18}$$

The ratio $|\varepsilon_{xc}(n,T)/\varepsilon_F| > |\varepsilon_x/\varepsilon_F| \approx 0.25r_s$ at low temperature and is only weakly dependent on temperature below T_F , so exchange-correlation effects are always significant up to the WDM regime. However, they become less important for $T > T_F$, where $\varepsilon_{xc}(n,T)/\varepsilon^0(n,T)$ decreases rapidly with increasing T. For the HEG, the exchange-correlation part of the chemical potential is equivalent to the DFT exchange-correlation potential $\mu_{xc}(n,T) \equiv v_{xc}(n,T)^{11}$ In our previous development,³⁰ we obtained results for $\varepsilon_{xc}(n,T)$ and $\mu_{xc}(n,T)$ over a broad range of temperatures and densities. In this followup we have significantly improved the precision of our calculations. This is particularly important at low T where the temperature dependence of $\varepsilon_{xc}(n,T)$ and $\mu_{xc}(n,T)$ is very weak. Fig. 2 shows a comparison of our updated results with the revised Karasiev et al. parameterization of QMC data, referred to below as KSDT. 20,21 These comparisons show that the accuracy of our present implementation of the FT RC Green's function approach is typically better than 10%, though it becomes worse at very low densities $r_s \approx 10$ or higher.

By definition the correlation energy is the difference between the total energy and that calculated in the

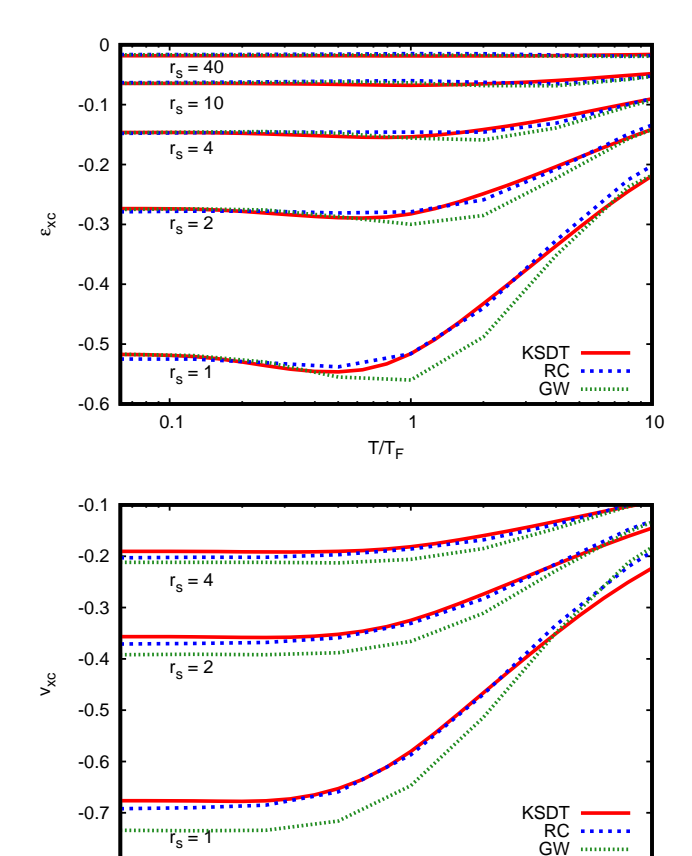


FIG. 2: (Color online) Finite-T exchange correlation parts of the energy per particle (Top) and chemical potential (Bottom) vs T/T_F for the HEG from the cumulant expansion (blue), the G^0W^0 Dyson approximation (green), and for comparison, the results of fits to QMC calculations (red). Note that these quantities scale roughly inversely with r_s .

T/T_F

-0.8

0.1

Hartree-Fock independent particle approximation, $E_c \equiv E_{xc} - E_x^0$. Thus the exchange and correlation energies per particle can also be separated unambiguously, as illustrated in Fig. 3. Note that the temperature dependence of $\varepsilon_{xc}(T)$ in Fig. 2 is very weak at low T, so that the much stronger temperature dependences of the exchange and correlation parts tend to cancel. Physically this cancellation is due to the screening of the Fock exchange operator, which otherwise would lead to singular behavior in the density of states and specific heat at $T = 0^+$.⁴⁰ Fig. 3 also shows that the $\varepsilon_x(T)$ decays rapidly above T_F , so that the WDM regime is dominated by Coulomb correlation effects, independent of spin.

D. Other approaches

1. Luttinger-Ward Approach

Analogous sum-rules in the $T \to 0^+$ limit were derived by Luttinger and Ward (LW) by exploiting the stationary property of the grand potential Ω with respect to variations in Σ .^{14,35} They obtain for the electron count

$$N^{LW}(\mu, T) = \sum_{k} \int d\omega \, D_k(\omega) f(\omega), \tag{19}$$

where the effective spectral function $D_k(\omega)$ is

$$D_k(\omega) = \frac{1}{\pi} \operatorname{Im} \frac{\partial \ln G_k(\omega)}{\partial \omega}.$$
 (20)

The difference between $A_k(\omega)$ and $D_k(\omega)$ can be understood from the identity $\partial \ln G_k/\partial \omega = -G(1-\partial \Sigma_k/\partial \omega)$.¹⁴ Remarkably, the sum and integral in Eq. (19) over $G_k(\omega)\partial\Sigma_k/\partial\omega$ vanishes at T=0 so that N^{LW} gives a count equivalent to that for N in Eq. (9). This difference is also reflected in the behavior of the satellites. The exact quasi-particle peak in $A_k(\omega)$ at $\varepsilon_k = \varepsilon_k^0 + \Sigma(k, \varepsilon_k)$ has a strength $Z_k = 1/(1 - \partial \Sigma_k/\partial \omega)$, while the remaining spectral weight is in the satellites. In contrast the quasiparticle peak at ε_k in $D_k(\omega)$ has strength unity and is infinitely sharp on the Fermi surface $k = k_F$, while the satellites have both positive and negative strengths. A consequence of this equivalence is that that satellites and quasi-particle renormalization effects cancel completely in the behavior of $N(\mu, T)$ and in the chemical potential $\mu(n,T)$ in the limit $T=0^+$. For this reason LW argue that their results for thermal properties at $T \to 0^+$ are exact and equivalent to those of a pure quasi-particle approximation.³⁸

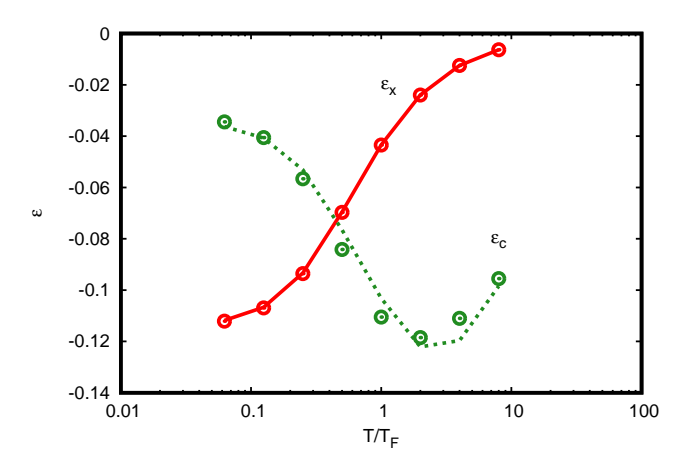


FIG. 3: (Color online) Comparison of exchange ε_x and correlation ε_c contributions to the the exchange-correlation energy per particle ε_{xc} vs T/T_F for the HEG at $r_s=4$ from the cumulant Green's function approach of this work (solid), and RPIMC data (circles).⁴

LW also show that renormalization effects cancel in the specific heat ratio which, as in Fermi liquid theory (FLT), is defined as $c_v/c_v^0 = m^*$ at $T \to 0^+$, where the effective mass $m^* = k_F/v_F$ is the only non-universal parameter of FLT.^{14,39} In particular, m^* is defined in terms of quasiparticle energy dispersion or the quasiparticle density of states $q^{qp}(\omega)$ at the Fermi level

$$m^* = \frac{k}{d\varepsilon_k/dk} \bigg|_{k=k_F} = \frac{\pi^2}{k_F} g^{qp}(\mu), \tag{21}$$

where the Fermi momentum $k_F = (3\pi^2 n)^{1/3}$. Although at T = 0, the Fermi momentum is not changed by manybody effects according to the Luttinger theorem, the Fermi surface is smeared by the Fermi function for T > 0 and not well defined. Moreover at $T \approx T_F$, the chemical potential lies below the lowest quasi-particle energy. It is therefore of interest to examine the validity of the LW results at finite T.

2. Quasiparticle approximation

In order to assess the importance of satellites and renormalization effects at finite T, it is useful to consider a pure quasi-particle (QP) approximation without these effects. In this paper the QP approximation refers to calculations with the spectral function $A_k^{qp}(\omega) = \delta(\omega - \varepsilon_k)$, where ε_k is the real part of the quasiparticle energy $\varepsilon_k = \varepsilon_k^0 + \Sigma_k(\varepsilon_k)$. Here $\Sigma_k(\omega)$ is taken to be the FT G^0W^0 approximation for the retarded GW self-energy defined above, although the QP energies could be taken from any approximation for the self-energy. The chemical potential can then be obtained by inverting the electron count in Eq. (9) with the QP spectral function $A_k^{qp}(\omega) = \delta(\omega - \varepsilon_k)$,

$$N^{qp}(\mu, T) = \sum_{k} f(\varepsilon_k) = V \int d\omega \, g^{qp}(\omega) f(\omega). \tag{22}$$

This alternative formula for $N(\mu, T)$ at T = 0 was also derived by LW. As a result, calculations of the chemical potential and other thermodynamic properties of the HEG greatly simplify, since a full frequency dependent self-energy is not required. Note that while the QP and FLT results for the chemical potential are identical at T=0, results for other quantities such as the total energy or specific heat are not the same. In particular FLT gives an exact result for the specific heat at T=0+ in terms of the exact quasi-particle energies due to the stationary properties of the Greens function at T=0.14,38 In contrast the QP approximation in this work refers to an explicit approximation for the spectral function, and the accuracy of results depend on the property being calculated, and how it is calculated. For example, the QP approximation within the Galitskii-Migdal-Koltun sum rule does not give accurate results for the total energy even at T=0. Fig. 4 shows a comparison of the chemical

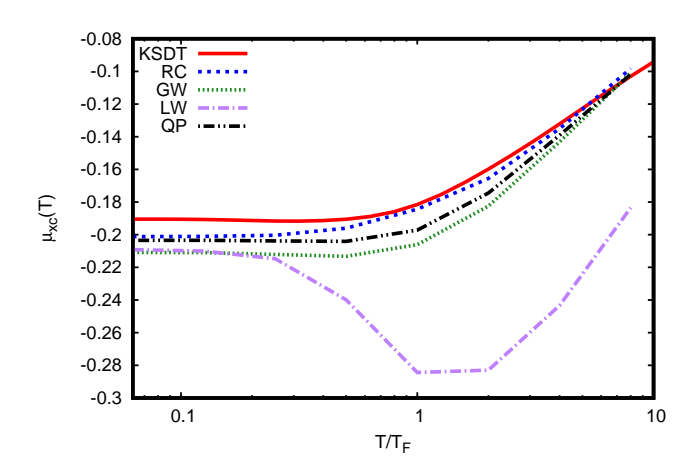


FIG. 4: (Color online) Exchange-correlation part of the chemical potential vs T/T_F at $r_s=4$, as calculated using the RC (blue), GW (green), LW (violet), and QP (black) spectral functions, and compared to the KSDT fit (red). 20,24

potential from the QP, RC and GW, and LW spectral functions, as well as the KSDT fit to QMC data. While the RC is closest to KSDT over the range studied, the QP approximation gives results that are bracketed by GW and RC over a large range of temperatures. However, the LW approach based on Eq. (19) rapidly loses accuracy with increasing temperature. The fairly good agreement between QP and RC shows that satellites and quasi-particle renormalization effects are largely, though not completely suppressed at finite T for calculations of the chemical potential. On the other hand, we find that using the QP approximation in the GMK sum-rule for $E(\mu,T)$ is less satisfactory, with errors of order 25%. Consequently the QP approximation is reasonable only for some pathways to thermodynamic quantities.

III. THERMODYNAMIC PROPERTIES

A. Chemical potential and energy per particle

Due to the exact separation of independent particle and exchange-correlation parts, one can regard the exchange-correlation contributions as those from an independent thermodynamic system, i.e., an exchange-correlation hole. Thus the contributions from the independent particle and exchange-correlation parts are additive and can be calculated and/or tabulated separately. By inverting Eq. (9) for $N(\mu, T)$ we obtain the Gibbs free energy per particle $\mu(n,T) = G/N$. Then subtracting the independent particle contribution, we obtain $\mu_{xc}(n,T)$. Next using this result for $\mu(n,T)$ in Eq. (12) and subtracting the independent particle part $\varepsilon^0(n,T)$ yields the exchange-correlation energy per particle $\varepsilon_{xc}(n,T)$. These calculations are carried out with our cumulant Green's function and the G^0W^0 approxi-

mation for the self-energy. 30 In this paper, $\mu_{xc}(n,T)$ and $\varepsilon_{xc}(n,T)$ have been recalculated with improved precision, particularly in the low temperature regime, since great numerical care is needed to avoid the near singular behavior of the calculations. Our results, as illustrated in Fig. 2, are typically accurate to better than about 10% compared to QMC fits of KSDT. Various thermodynamic properties can then be derived in terms of $\mu(n,T)$ and/or $\varepsilon(n,T)$ using thermodynamic identities.

B. Helmholtz free energy and electron pressure

The Helmholtz free energy F=E-TS can be obtained by numerical integration. First, keeping the electron density n fixed and using the identity⁵⁶ $\partial [F(n,T)/T]/\partial T=E(n,T)/T^2$, the free energy density per particle f=F/N is given by a high temperature integration

$$f(n,T) = \frac{T}{T'}f(n,T') - T\int_{T'}^{T} d\tau \, \frac{\varepsilon(\tau,n)}{\tau^2},\tag{23}$$

where T' is a suitably high temperature above which the asymptotic form $f_{\rm xc}(T) \to -(3T)^{-1/2} r_s^{-3/2}$ is valid.⁵⁷ Despite the singular factor $1/\tau^2$ in the integrand, if the zero temperature energy is subtracted, the integral to obtain $\bar{f}(T) = f(T) - f(0)$ is well behaved when $T \to 0^+$. The reason is that $\bar{\varepsilon}(n,T) \equiv \varepsilon(n,T) - \varepsilon(0,n)$ vanishes at T=0 due to the linear behavior of the specific heat, $\bar{\varepsilon}(n,T) \to (1/2)\gamma(n)T^2, \ (T \to 0^+)$. Alternatively, one can obtain f(n,T) by integrating the chemical potential over the electron density (or r_s) at low density keeping V and T fixed, using the relation $\mu = \partial(F/V)/\partial n$ with $n(r) = 3/4\pi r^3$,

$$f(n,T) = 3r_s^3 \int_{r_s}^{\infty} dr \, \frac{\mu(n(r),T)}{r^4}.$$
 (24)

This formula is the FT generalization of a similar expression for the ground state energy per particle $\varepsilon(n,0) =$ f(n,0). ^{55,58} Results for these two pathways for obtaining $f_{xc}(n,T)$ are compared in Fig. 5 for $r_s=4$. Note that these results for $f_{xc}(n,T)$ differ by a small, approximately constant shift, of about 0.013 Hartree. This discrepancy suggests that our cumulant Green's function based on the G^0W^0 self-energy is not fully self-consistent or conservative. Similarly, as discussed by Holm, ⁵⁹ the lack of partial or full self-consistency in GW calculations at T=0 also leads to nearly constant shifts in the chemical potential resulting from different formulae. Consequently, some level of self-consistency, such as the quasiparticle selfconsistent GW (QPSCGW) approximation may be an improvement for some quantities.³⁶ However, a detailed treatment of self-consistency in the cumulant expansion has not yet been developed, and is therefore beyond the scope of the present work.

Nevertheless, the above discrepancy does not imply a serious limitation of our current approach. Clearly the result based on the high-temperature integration of

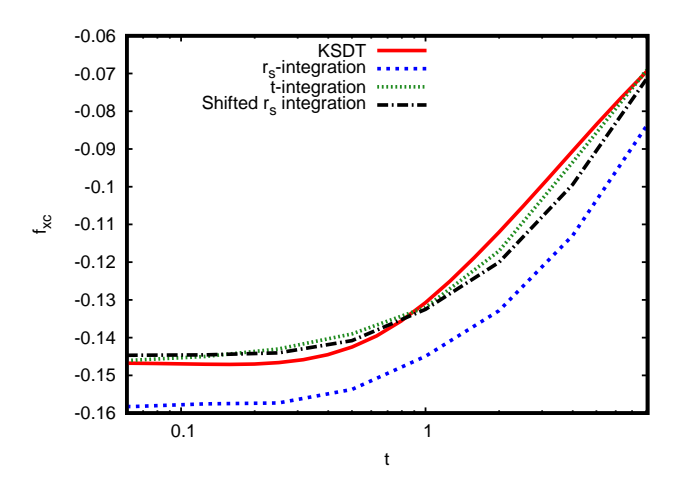


FIG. 5: (Color online) Exchange correlation part of the Helmholtz-free energy calculated via an integration over temperature (green) compared with that calculated via integration over r_s (blue), and the KSDT (red). 20,24 The black curve shows the r_s form shifted by a constant 0.013 Hartree.

 $\varepsilon(n,T)/T^2$ from the GMK sum rule matches more closely to QMC results, and is therefore a preferred prescription. This choice is also justified on physical grounds since the density integration path depends on the chemical potential at very low densities where correlation effects are strongest and the cumulant approach least reliable. As an alternative prescription, the discrepancy in the density integration path can be accounted for simply by adding a shift so that f(n,T) matches to the ground state energy per particle at T=0. As shown in Fig. 5 both of these prescriptions yield very good agreement with QMC.

Given f(n,T) and $\mu(n,T)$, the electron pressure can be obtained from the relation $\Omega = -pV = (F - G)$, i.e.,

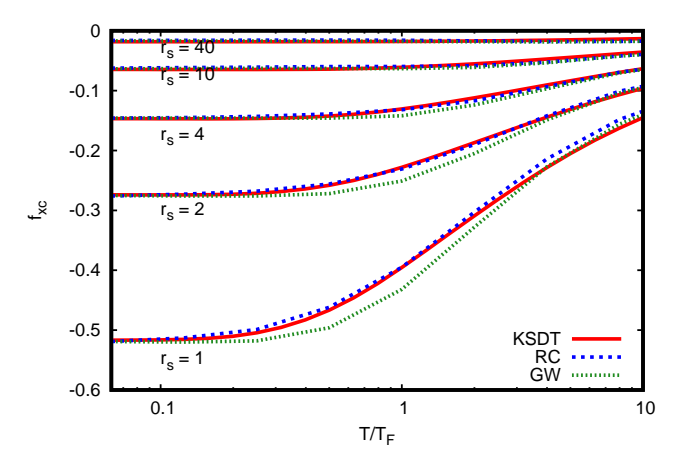
$$p(n,T) = n[\mu(n,T) - f(n,T)].$$
 (25)

A decomposition into independent particle and exchangecorrelation parts similar to those for ε and μ applies to all derived thermodynamic potentials and densities, so

$$f(n,T) = f^{0}(n,T) + f_{xc}(n,T),$$
 (26)

$$p(n,T) = p^{0}(n,T) + p_{xc}(n,T).$$
 (27)

The exchange-correlation contributions to the Helmholtz free energy per particle f_{xc} , and the electron pressure p_{xc} for the HEG are shown in Fig. 6. The accuracy of the calculation of p_{xc} is less than that of f_{xc} due to the subtraction in Eq. (25), and depends on how f_{xc} and μ_{xc} are calculated. We note that $p^0(n,T)=(2/3)n\varepsilon^0(n,T)$ for all n and T and asymptotes to the classical limit $p\to nk_BT$ at high T (see Fig. 7). The exchange-correlation pressure $p_{xc}(n,T)$ corresponds to the generalization of the Fermior exchange-pressure due to the Pauli principle. At low T this contribution is dominated by exchange, and at high T by correlation contributions. However, in contrast to the dominance of the Fermi pressure at T=0, the exchange-correlation effects are both small compared to the independent particle pressure for $T>>T_F$.



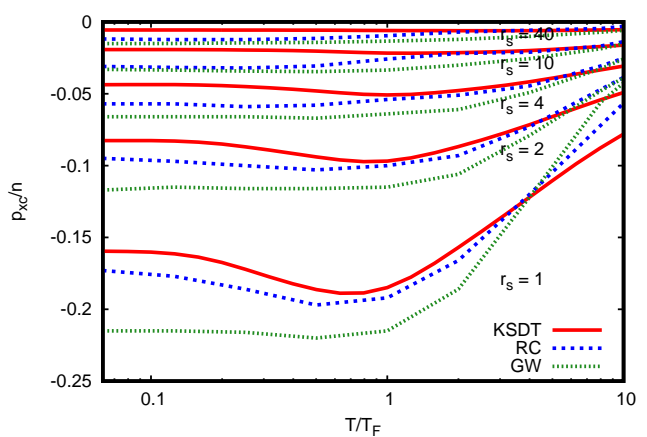


FIG. 6: (Color online) Exchange-correlation contributions to the Helmholtz-free energy per particle f_{xc} (top) and the electron pressure p_{xc} (bottom) vs T/T_F for the the HEG from the retarded cumulant Green's function approach (RC, blue)³⁰, compared to those from GW (green) and the KSDT fit (red). Note that the RC generally agrees better than GW with the KSDT fits.

C. Entropy and Specific Heat

Of long-standing interest in many-body theory is the behavior of the entropy per particle s=S/N and constant volume specific heat c_v of interacting Fermi-systems. In the low temperature limit $T\to 0^+$, both s(n,T) and $c_v(n,T)$ are linear in temperature and equal, i.e., $c_v(n,T)=T\partial s(n,T)/\partial T=s(n,T)\equiv \gamma(n)T$. The ratio $c_v/c_v^0=\gamma/\gamma^0=m^*$ then corresponds to the effective mass $m^*=k_F/v_F$ defined in Eq. (21). However, values of m^* for the HEG have been notoriously difficult to pin down definitively. ^{18,60} Likewise there is a currently a lack of accurate QMC data at very low T which could help resolve this issue. To our knowledge, however, the behavior of the specific heat in the WDM regime has not been extensively investigated.

In an effort to investigate this behavior we first evaluate the entropy per particle s(n,T) using the relation $Ts = \varepsilon - f$ with a high temperature integration for f.

The exchange correlation part is then obtained by subtracting Ts^0 , and similarly for $c_v = T\partial s/\partial T$,

$$s(n,T) = s^{0}(n,T) + s_{xc}(n,T),$$
 (28)

$$c_v(n,T) = c_v^0(n,T) + c_{vxc}(n,T).$$
 (29)

Results for the exchange-correlation entropy per particle s_{xc} are shown in Fig. 8. Remarkably entropic effects on the exchange-correlation contributions are only substantial at relatively high T of order T_F . This behavior reflects the cross-over from exchange- to correlationdominated behavior in WDM where spin can be ignored.

Our results for the specific heat are illustrated in Fig. 9. First (Top), we compare those at T=0 for $c_v/c_v^0=m^*$ from Eq. (21), to calculations based on Fermi liquid theory as in Eq. (21), the RPA, 55,61 and the KSDT parameterization. Note that the RC results more closely match those from the KSDT fits to QMC. However, they are slightly higher than those of Fermi liquid (FLT) or the RPA. Next (Bottom), we compare the temperature dependence of $c_v(T)/c_v^0(T)$ to KSDT. Although both curves exhibit an oscillatory behavior, the minima and maxima in the RC calculation occur at higher temperatures. The value of γ at T=0 also fixes the leading quadratic temperature variation of the energy and the Helmholtz free energy,

$$\varepsilon(n,T) = \varepsilon(n,0) + (1/2)\gamma T^2 + \cdots, \qquad (30)$$

$$f(n,T) = \varepsilon(n,0) - (1/2)\gamma T^2 + \cdots$$
 (31)

Similarly the density dependence of $\gamma(n)$ determines the leading quadratic behavior of the chemical potential. From the relation $(\partial \mu/\partial T)_n = -(\partial s/\partial n)_T$, we find

$$\mu = \mu(0) - \frac{1}{2} \frac{d\gamma(n)}{dn} T^2 + \cdots$$
 (32)

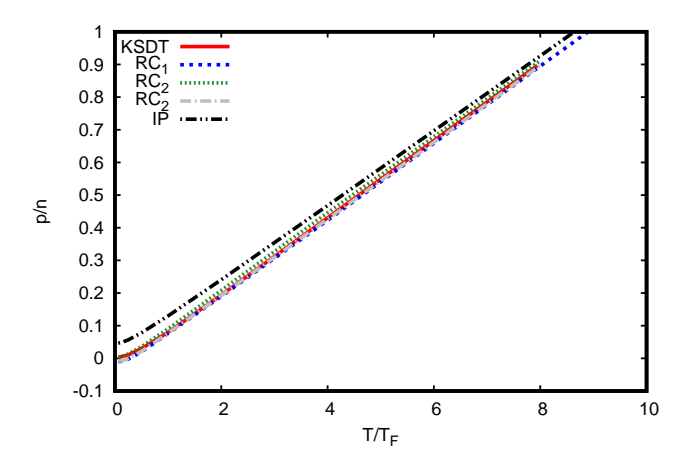


FIG. 7: (Color online) Electron pressure p(n,T)/n compared to the independent particle result for the HEG at $r_s=4$ from the RC (blue), IP (green), and from KSDT fits (red). Note that the effect of exchange and correlation is significant for $T < T_F$ but relatively small for $T >> T_F$.

Nevertheless, this quadratic behavior does not persist at higher T where the Fermi surface broadens over a width of order k_BT . For example, in the quasi-particle approximation, the low T specific heat corresponds to an average of the density of states $g^{qp}(\omega)$ over this smeared Fermi surface. From the negative curvature of $g^{qp}(\omega)$ near $\omega \approx \mu$ in Fig. 1, one expects a reduction in the magnitude of c_v/c_v^0 with increasing T near T=0, as observed in the lower part of Fig. 9. These results suggest that the ratio $c_v(T)/c_v^0(T)$ has a minimum at some temperature below T_F . This is roughly consistent with the variations seen in the KSDT fit to QMC data at low temperature. However, the ratio is difficult to estimate with precision numerically, as $c_v(T)$ and $c_v^0(T)$ are both very small at low T.²⁴

D. Isothermal compressibility

Another quantity of interest is the isothermal compressibility κ , which is related to the density fluctuations in the system and can be obtained from the density dependence of the chemical potential

$$\kappa(n,T) = -\frac{1}{\partial \mu(n,T)/\partial n} = 4\pi \frac{r_s^2}{\partial \mu/\partial r_s}.$$
 (33)

Results for $\kappa(n,T)$ are shown in Fig. 10, where the low temperature results are seen to be in good agreement with those from QMC and many-body perturbation theory, including vertex corrections.¹⁸

IV. SPIN-POLARIZED ELECTRON GAS

We conclude our derivation of thermodynamic properties with a brief discussion of spin-dependent contribu-

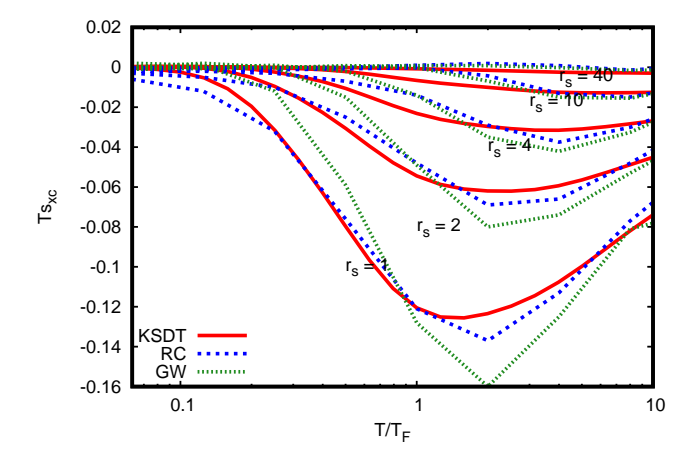


FIG. 8: (Color online) Exchange-correlation contributions $s_{xc}(n,T)$ to the entropy per particle, scaled by temperature T at various densities for the HEG from RC (blue), GW (green), and KSDT (red).

tions. Spin-polarization is important in many contexts in condensed matter, especially in magnetism. Here we assume for simplicity that electrons with different spins can be treated independently. For example, in the HEG electrons of each spin $\sigma = \pm 1/2$ are uniformly distributed with fixed spin-dependent equilibrium number densities n_{\pm} where $n = (n_{+} + n_{-}) = N/V$ is the total number density. By defining the degree of spin polarization as $\chi = (n_+ - n_-)/n$, and $n = (4\pi r_s^3/3)^{-1}$ where r_s is the Wigner-Seitz density parameter, the finitetemperature spin dependent interacting electron gas can be described by three parameters χ , T and r_s . We also define the dimensionless spin-dependent reduced temperatures $\tau_{\sigma} \equiv T/T_F^{\sigma}$, where $T_F^{\sigma} = \varepsilon_F^{\sigma}/k_B$ is the Fermi temperature for the spin- σ electrons in the gas.

The thermodynamics of the spin-dependent system can then be treated analogously to the unpolarized system, substituting the spin-dependent quantities respectively. For example calculations of the spin dependent energy

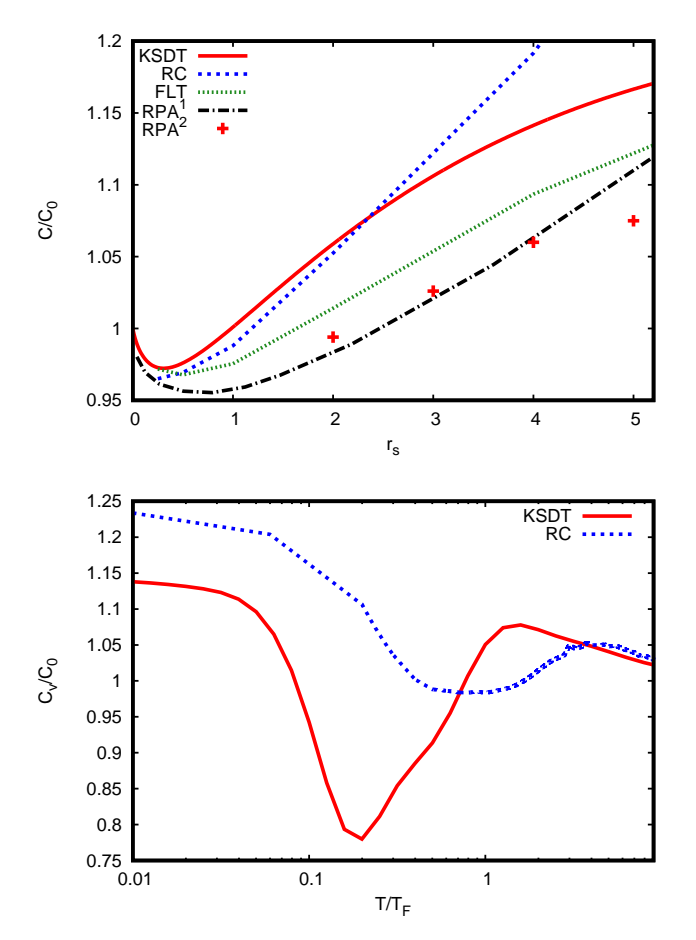


FIG. 9: (Color online) Top: Specific heat ratio c_v/c_v^0 vs density parameter r_s and T=0 for the HEG from the GMK sumrule using RC (blue) compared with m^* of Fermi liquid theory (FLT) (green), the RPA calculation of Lundqvist (black)⁵⁵ and of Louie et al. (red crosses).⁶¹ Bottom: Temperature dependence $c_v(T)/c_v^0(T)$ for $r_s = 4$ from RC (blue) compared with the KSDT fit (red).

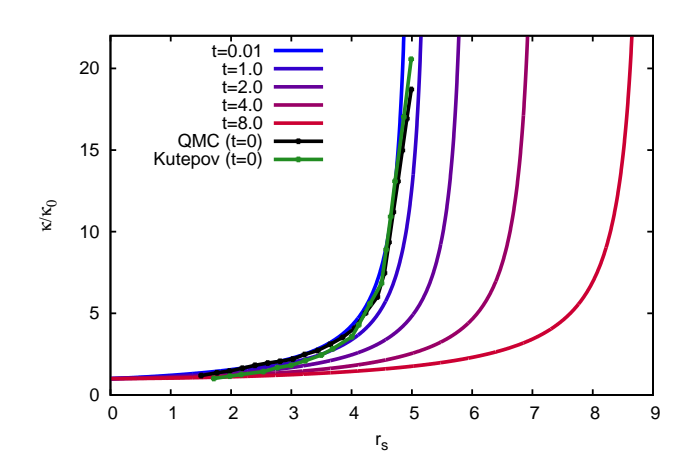


FIG. 10: (Color online) Isothermal compressibility of the HEG vs density parameter r_s at various temperatures t = T/T_F . For comparison results from QMC and GWF-MBPT at T = 0 are also given.¹⁸

per particle $\varepsilon_{\sigma}(T) = E_{\sigma}(T)/N$ are again calculated with the spin-dependent generalization of GMK sum-rule, i.e., with a spin-dependent spectral function $A_{k\sigma}(\omega)$ as in Eq. (1). Likewise, each spin population has a chemical potential fixed by the spin-dependent densities n_{σ} and Fermi factors $f_{\sigma}(\varepsilon) = 1/[e^{\beta(\varepsilon-\mu_{\sigma})} + 1]$. The spin-dependent self-energies are again approximated by the GW approximation at the G^0W^0 level, but with implicit temperature and spin dependence in the Fermi- and Bose-factors. The exchange-correlation parts are also defined analogously, by subtracting the independent particle contributions. Results for the energy and chemical potential vs T for full polarization $\chi = 1$ are shown in Fig. 11.

Similarly, the spin-dependent Helmholtz free-energies $F_{\sigma}(T)$ can again be calculated by integrating $E_{\sigma}(T)/T^2$ as in Eq. (12). Thus the total Helmholtz F and Gibbs free energies G can be expressed as as sum over spindependent contributions

$$F = \sum_{\sigma} F_{\sigma} = \sum_{\sigma} N_{\sigma} f_{\sigma}(T) \tag{34}$$

$$F = \sum_{\sigma} F_{\sigma} = \sum_{\sigma} N_{\sigma} f_{\sigma}(T)$$

$$G = \sum_{\sigma} G_{\sigma} = \sum_{\sigma} N_{\sigma} \mu_{\sigma}(T)$$
(34)

Similarly the pressure can be obtained from the thermodynamic potential $\Omega = F - G = -V \Sigma_{\sigma} p_{\sigma}(T)$, so

$$p = \sum_{\sigma} n_{\sigma} [\mu_{\sigma} - f_{\sigma}]. \tag{36}$$

Results for f_{xc} and p_{xc} based on high temperature integration and matched to the limiting forms

$$f_{\rm xc}(T) \rightarrow -(3T)^{-1/2}r_s^{-3/2} + O(T^{-1}),$$
 (37)

$$\varepsilon_{\rm xc}(T) \rightarrow -(1/2)(3T)^{-1/2}r_s^{-3/2} + O(T^{-1})., (38)$$

are shown in Fig. 12. These results are independent of both σ and χ .⁵⁷

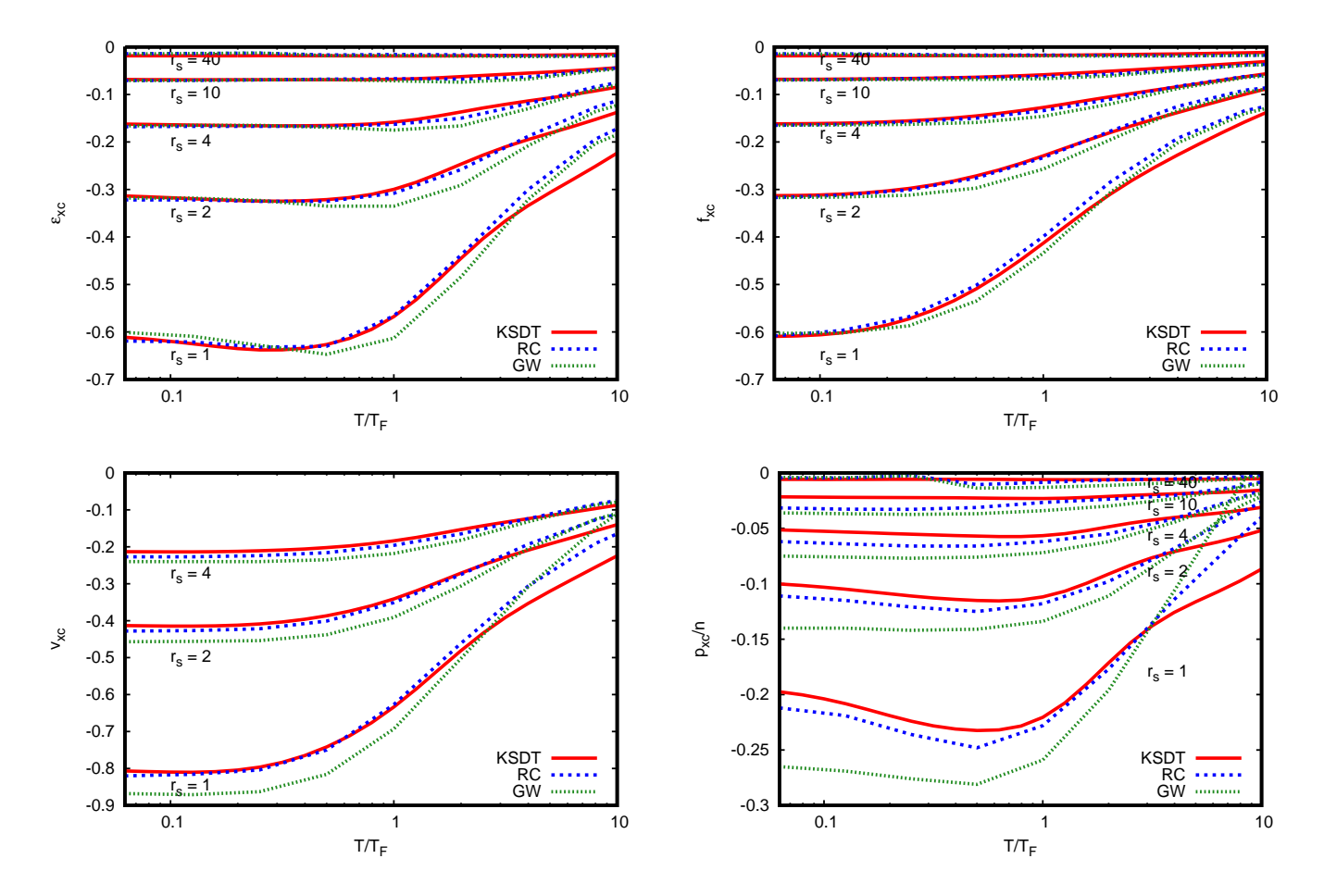


FIG. 11: (Color online) Finite-T exchange correlation parts of the energy per particle (Top) and chemical potential (Bottom) vs $\tau = T/T_F$ for the spin-polarized HEG with $\chi = 1$ from the cumulant Green's function (blue), compared with GW (green) and KSDT (red) results.

FIG. 12: (Color online) Exchange-correlation parts of the Helmholtz free energy per particle f_{xc} (Top) and electron pressure p_{xc} (Bottom), vs $\tau = T/T_F$ for the spin-polarized HEG with $\chi = 1$ from the cumulant expansion (blue), GW (green), and KSDT (red).

V. SUMMARY AND CONCLUSIONS

We have presented calculations of a number of thermodynamic properties of the interacting HEG including optional spin-polarization over a wide range of densities and temperatures up to the warm dense matter regime $T \sim T_F$. Our approach is based on the many-body formalism of MS with a FT extension of retarded cumulant Green's function and sum rules for the total electron number and energy. This approach permits a quantitative analysis of exchange and correlation contributions to the thermodynamics, and consequently provides an alternative source of data for the electron gas. Although the temperature and density dependence is implicit, the numerical results can be parameterized either to determine or to improve existing finite-temperature DFT exchangecorrelation functionals.^{8,20,21} We find that exchangecorrelation effects are slowly varying at low temperature $T < T_F$, but decrease rapidly in the WDM regime $T \geq T_F$ where exchange becomes small and Coulomb correlation dominates. Consequently at "cool" temperatures $(T \ll T_F)$ and normal densities $(2 \ll r_s \ll 6)$, conventional approaches such as Fermi liquid theory are good approximations. More generally, we find that the FT RC approach with a G^0W^0 self-energy is a very good approximation for a much wider range of temperatures, including the WDM regime. The RC approach generally improves on the GW and QP approximations, and is typically accurate to better than 10% compared to QMC, though the errors are larger at very low densities $r_s \sim 10.9$ Moreoer improvements are possible. It seems likely, for example, that part of the error is due to the non-conserving properties of the RC Green's function. These errors are reflected by the small discrepancies in quantities like the Helmholtz free energy calculated using different thermodynamic identities. This is a well known limitation of the G^0W^0 approach leading to similar discrepancies in the chemical potential,⁵⁹ which are cured for the most part by self-consistency. However, these discrepancies do not pose a serious limitation to our approach, since either a high-temperature integration or a

well defined shift both yield accurate results compared to QMC. Results for the entropy and specific heat are consistent with the predictions of Fermi liquid theory in the $T \to 0^+$ limit, but deviations are observed at higher temperatures, even well below T_F . Although the RC results for the specific heat ratio $c_v/c_v^0 = m^*$ are closer to those from QMC, especially at high densities, they are somewhat larger than other methods, and there is a need for more quantitative treatments to resolve the differences. We also find that satellites and quasi-particle renormalization effects are largely but not completely suppressed at finite T for some quantities, though not the total en-

ergy. Consequently, the QP approximation with a GW self-energy can sometimes be fairly good. Although the calculations presented here are restricted to thermodynamic properties the HEG, the retarded cumuant method is more generally applicable, and provides a systematic, first principles approach for calculations of many physical properties.

Acknowledgments: We thank G. Bertsch, V. Karasiev, A. Kutepov, G.D. Mahan, R. Martin, N.D. Mermin, D. Pemmaraju, L. Reining, and S. Trickey for comments and suggestions. This work is supported by DOE Office of Science BES Grant DE-FG02-97ER45623.

- ¹ M. Koenig, A. Benuzzi-Mounaix, A. Ravasio, T. Vinci, N. Ozaki, S. Lepape, D. Batani, G. Huser, T. Hall, D. Hicks, et al., Plasma Phys. Control. Fusion 47, B441 (2005).
- ² S. Glenzer, H. Lee, P. Davis, T. Döppner, R. Falcone, C. Fortmann, B. Hammel, A. Kritcher, O. Landen, R. Lee, et al., High Energy Density Physics 6, 1 (2010).
- ³ K. P. Driver and B. Militzer, Phys. Rev. B **93**, 064101 (2016).
- ⁴ E. W. Brown, B. K. Clark, J. L. DuBois, and D. M. Ceperley, Phys. Rev. Lett. **110**, 146405 (2013).
- ⁵ G. G. Spink, R. J. Needs, and N. D. Drummond, Phys. Rev. B 88, 085121 (2013).
- ⁶ S. Tanaka and S. Ichimaru, J. Phys. Soc. Jpn. **55**, 2278 (1986).
- ⁷ T. Dornheim, S. Groth, T. Sjostrom, F. D. Malone, W. M. C. Foulkes, and M. Bonitz, Phys. Rev. Lett. 117, 156403 (2016).
- ⁸ S. Groth, T. Dornheim, T. Sjostrom, F. D. Malone, W. M. C. Foulkes, and M. Bonitz, Phys. Rev. Lett. **119**, 135001 (2017).
- ⁹ T. Dornheim, S. Groth, and M. Bonitz, Phys. Reports **744**, 1 (2018).
- P. Hohenberg and W. Kohn, Phys. Rev. 136, B864 (1964).
- ¹¹ W. Kohn and L. J. Sham, Phys. Rev. **140**, A1133 (1965).
- ¹² N. D. Mermin, Phys. Rev. **137**, A1441 (1965).
- ¹³ R. M. Martin, L. Reining, and D. M. Ceperley, *Interacting Electrons, Theory and Computational Approaches* (Cambridge University Press, Cambridge, 2016).
- A. Abrikosov, L. Gorkov, I. Dzyaloshinski, and R. Silverman, Methods of Quantum Field Theory in Statistical Physics (Dover Publications, New York, 2012).
- ¹⁵ G. Mahan, Many-Particle Physics (Springer, 2000).
- ¹⁶ M. W. C. Dharma-wardana, J. Phys.: Conf. Ser. 442, 012030 (2013).
- $^{17}\,$ S. Hong and G. D. Mahan, Phys. Rev. B ${\bf 53},\,1215$ (1996).
- ¹⁸ A. L. Kutepov and G. Kotliar, Phys. Rev. B **96**, 035108 (2017).
- ¹⁹ K. Burke, J. C. Smith, P. E. Grabowski, and A. Pribram-Jones, Phys. Rev. B **93**, 195132 (2016).
- V. V. Karasiev, T. Sjostrom, J. Dufty, and S. B. Trickey, Phys. Rev. Lett. 112, 076403 (2014), see especially supplementary materials.
- ²¹ V. V. Karasiev, L. Calderín, and S. B. Trickey, Phys. Rev. E **93**, 063207 (2016).
- ²² Z. Yan, J. P. Perdew, and S. Kurth, Phys. Rev. B 61,

- 16430 (2000).
- ²³ K. S. Singwi, M. P. Tosi, R. H. Land, and A. Sjölander, Phys. Rev. **176**, 589 (1968).
- ²⁴ V. V. Karasiev, S. B. Trickey, and J. W. Dufty, Phys. Rev. B **99**, 195134 (2019).
- ²⁵ J. J. Rehr and J. J. Kas, Eur. Phys. J. B **91**, 153 (2018).
- ²⁶ S. Groth, T. Dornheim, and J. Vorberger, Phys. Rev. B 99, 235122 (2019).
- ²⁷ N. W. Ashcroft and N. D. Mermin, Solid State Physics (Holt, Rinehart and Winston, 1976).
- ²⁸ F. Giustino, Rev. Mod. Phys. **89**, 015003 (2017).
- ²⁹ P. C. Martin and J. Schwinger, Phys. Rev. **115**, 1342 (1959).
- ³⁰ J. J. Kas and J. J. Rehr, Phys. Rev. Lett. **119**, 176403 (2017).
- ³¹ D. S. Koltun, Phys. Rev. C **9**, 484 (1974).
- ³² S. Engelsberg and J. R. Schrieffer, Phys. Rev. **131**, 993 (1963).
- ³³ P. B. Allen and B. Mitrović, in *Solid State Physics*, edited by H. Ehrenreich, F. Seitz, and D. Turnbull (Academic Press, 1982), vol. 37, pp. 1–92.
- ³⁴ P. Allen and V. Heine, J. Phys. C **9**, 2305 (1976).
- ³⁵ J. M. Luttinger and J. C. Ward, Phys. Rev. **118**, 1417 (1960).
- ³⁶ S. V. Faleev, M. van Schilfgaarde, T. Kotani, F. Léonard, and M. P. Desjarlais, Phys. Rev. B 74, 033101 (2006).
- ³⁷ C.-O. Almbladh, U. von Barth, and R. van Leeuwen, Intl.
 J. Mod. Phys. B 13, 535 (1999).
- ³⁸ J. M. Luttinger, Phys. Rev. **119**, 1153 (1960).
- ³⁹ L. Landau, Soviet Phys. JETP **3**, 920 (1956).
- ⁴⁰ L. Hedin, J. Phys.: Condens. Matter **11**, R489 (1999).
- ⁴¹ J. J. Kas, F. D. Vila, J. J. Rehr, and S. A. Chambers, Phys. Rev. B **91**, 121112(R) (2015).
- ⁴² J. J. Kas, J. J. Rehr, and J. B. Curtis, Phys. Rev. B **94**, 035156 (2016).
- ⁴³ J. Lischner, D. Vigil-Fowler, and S. G. Louie, Phys. Rev. B **89**, 125430 (2014).
- ⁴⁴ F. Caruso, H. Lambert, and F. Giustino, Phys. Rev. Lett. 114, 146404 (2015).
- ⁴⁵ F. Caruso and F. Giustino, Phys. Rev. B **92**, 045123 (2015).
- ⁴⁶ D. C. Langreth, Phys. Rev. B **1**, 471 (1970).
- ⁴⁷ J. J. Kas, J. J. Rehr, and L. Reining, Phys. Rev. B **90**, 085112 (2014).
- ⁴⁸ J. Zhou, J. Kas, L. Sponza, I. Reshetnyak, M. Guzzo, C. Giorgetti, M. Gatti, F. Sottile, J. Rehr, and L. Reining,

- J. Chem. Phys. 143 (2015).
- ⁴⁹ T. S. Tan, J. J. Kas, and J. J. Rehr, Phys. Rev. B **98**, 115125 (2018).
- ⁵⁰ L. Landau, J. Phys. USSR **8**, 201 (1944).
- ⁵¹ U. von Barth and B. Holm, Phys. Rev. B **54**, 8411 (1996).
- ⁵² F. C. Khanna and H. R. Glyde, Can. J. Phys. **54**, 648
- ⁵³ N. R. Arista and W. Brandt, Phys. Rev. A **29**, 1471 (1984).
- 54 G. Baym and L. P. Kadanoff, Phys. Rev. $\boldsymbol{124},\,287$ (1961).
- 55 B. I. Lundqvist, Phys. kondens. Materie ${\bf 6},\,206$ (1967).
- ⁵⁶ M. Dharma-wardana and R. Taylor, J. Phys. C: Solid State

- Phys. 14, 629 (1981).
- ⁵⁷ H. E. DeWitt, J. Math. Phys. **7**, 616 (1966).
- ⁵⁸ F. Seitz, *Modern Theory of Solids* (McGraw-Hill Book Company Inc, New York, 1940).
- ⁵⁹ B. Holm, Phys. Rev. Lett. **83**, 788 (1999).
- 60 F. G. Eich, M. Holzmann, and G. Vignale, Phys. Rev. B
- 96, 035132 (2017).

 Graph J. E. Northrup, M. S. Hybertsen, and S. G. Louie, Phys. Rev. B **39**, 8198 (1989).